12th Brazilian Congress of Manufacturing Engineering
May 10th-12th, 2023, Brasilia, DF, Brazil

EXPERIMENTAL STUDY OF MICROMILLING OF DIRECTED ENERGY DEPOSITED H13 TOOL STEEL

Milla Caroline Gomes
Federal University of Uberlândia, School of Mechanical Engineering, Campus Santa Mônica – Uberlândia – MG, Brazil
millagomes@ufu.br

Márcio Bacci da Silva
Federal University of Uberlândia, School of Mechanical Engineering, Campus Santa Mônica – Uberlândia – MG, Brazil
mbacci@ufu.br

Wayne NP Hung
Texas A&M University, Engineering Technology & Industrial Distribution Department, College Station, Texas, USA
hung@tamu.edu

Reginaldo Teixeira Coelho
University of Sao Paulo, Sao Carlos School of Engineering, Department of Production Engineering, Sao Carlos – SP, Brazil
rtcoelho@sc.usp.br

Abstract. *Parts manufactured by additive manufacturing (AM) processes have rough surface finish and poor dimensional accuracy, therefore, post-processing must be required. Among the post-processing techniques, micro-milling is popular because it can enhance surface quality and geometric inaccuracies, while being applicable to a wide variety of additive manufactured metals. Since machinability of materials manufactured by AM differs from those manufactured conventionally, this work investigates the micromilling of AISI H13 tool steel manufactured by the laser-beam directed energy deposition (LDED) process and compares it with the micromilling of the same steel obtained by hot rolling and annealing heat treatment. Both quality of the machined surface and the cutting force were analyzed to assess the machinability. The force signals were acquired using a Kistler dynamometer and signal amplifier, together with a National Instruments acquisition board and a computer with LabView Signal Express software. Roughness of a micromilled channel was measured using a Taylor Hobson profilometer. Micromilling was performed with the Minitech micromilling system with a maximum speed of 60,000 rpm. Mitsubishi (Al,Ti)N coated carbide tool, with a cutting diameter of 400 µm and two cutting flutes were used. The cutting parameters included a cutting speed of 12.6 m/min, feed per tooth of 10 µm/tooth, axial depth of cut of 40 µm and radial depth of cut equal to 400 µm. Longer milling time caused a reduction of surface roughness Ra and an increase in the cutting force. No statistically significant differences between the Ra values and the cutting force were obtained for micromilling the hot-rolled versus LDED samples. However, the wear results of the microtools were compatible with the differences in the hardness of the analyzed samples.*

Keywords: *micromilling; additive manufacturing; H13 tool steel; directed energy deposition.*

1. INTRODUCTION

Micromilling is an important micromachining process that has been widely used because it allows the manufacture of complex geometries with high precision on many materials (Serje et al., 2020). Due to these characteristics, micromilling has been used as a post-processing technique for materials manufactured by additive manufacturing, precisely because it can enhance both surface quality and geometric inaccuracies (Salonitis et al., 2016; Gomes et al., 2021).

In micromilling, the dimensions of the cutting tools vary from 1 µm to 1000 µm (Aramcharoen et al., 2008; Câmara et al., 2012). Rodrigues and Jasinevicius (2017), claimed that in this process, the dimensions involved are on the micrometric scale and defined the range of some of the process variables that correspond to cutting on a micro-scale. The values that have been set are:

I. Uncut chip thickness: 5 µm ~ 20 µm;
II. Axial depth of cut: 1 µm ~ 100 µm;
III. Tool edge radius: 1 µm ~ 5 µm.

Therefore, it is noted that there is no consensus regarding the definition of the micromilling process, which is incomplete when considering only the values of the process variables or the diameter of the microtool. This difficulty is related to the specific phenomena that occur in micromachining, explained by the size effect. Therefore, it is not an easy

task to establish a limit, from which the presence of the scale effect will have a greater influence (Simoneau et al., 2006). Thus, it is suggested that the concept to be given regarding micromilling should be a combination of the mentioned concepts since one would complement others.

The presence of the size effect is characterized by the significant increase in the specific energy, from the reduction of the uncut chip thickness (Liu and Melkote, 2007). This phenomenon explains the mechanisms that occur in micromilling, due to scale reduction in relation to macro-scale milling. This effect is present when the uncut chip thickness becomes comparable to the radius of the cutting edge and the grain of the machined material. Therefore, in micromilling, the grain size of the material, the uncut chip thickness, and the radius of the cutting edge have a great influence on the process (Cheng and Huo, 2013).

Additive manufacturing processes are being increasingly used as they enable the manufacture of complex geometries (Zhai et al., 2014). However, parts manufactured by these processes usually have a low surface finish and dimensional accuracy. Thus, after manufacturing these parts, they are subjected to post-processing techniques, such as micromilling, with the aim of improving surface quality and dimensional accuracy (Kumbhar and Mulay, 2018).

Of the additive manufacturing processes, those used in the manufacture of metallic parts are binder jetting (BJ), sheet lamination (SL), directed energy deposition (DED), and powder bed fusion (PBF) among which the last two are mostly used (Zhang et al., 2018). The popular DED is developed for different metals, and repairing damaged or worn parts (Yi et al., 2019).

In general, the machinability of AM metals differs from the same metals manufactured by conventional methods, with metals obtained by additive manufacturing having lower machinability (Hung and Corliss, 2019). Therefore, it becomes important to investigate the main differences between micromilling of conventional materials and those manufactured by additive manufacturing. This work aims to carry out an experimental study to investigate the micromilling of AISI H13 tool steel manufactured by hot rolling and by DED.

2. METHODOLOGY

The workpiece used in carrying out the tests was AISI (American Iron and Steel Institute) H13 tool steel manufactured by LDED. The H13 tool steel is commonly used for high temperature die and mold as in hot forming or injection molding (Asnafi, 2021).

The chemical composition in the percentage of the weight of the two analyzed samples is shown in Table 1. The composition of the hot rolling sample was obtained by the Materials Testing and Analysis Laboratory – LAMAT of SENAI Itaúna, while that of the LDED sample was obtained by EDS using the SEM from Hitachi High-Technologies®, TM3000. Note that the difference in the amount of carbon is due to the inaccuracy of the SEM system in detecting this chemical element.

Table 1. Chemical composition of AISI H13 tool steel (LAMAT and EDS).

H13	Chemical composition (wt%)										
	C	Si	Mn	P	S	Cr	Mo	Al	Cu	Ni	V
Hot-Rolled	0.380	0.910	0.300	0.010	0.005	5.090	1.270	0.010	0.080	0.310	0.850
LDED	8.155	1.128	0.431	0.081	-	5.286	1.049	0.019	0.004	-	0.745

Table 2 shows the hardness of each analyzed sample.

Table 2. AISI H13 tool steel hardness.

H13	Hardness (HV)
Hot-rolled	204
LDED	513

The micromilling tests, for the manufacture of 10 microchannels in each analyzed 13x12x5 mm sample, were carried out on a CNC Mini-mill/GX model micromilling machine, manufactured by Minitech Machinery Corporation®, which has a maximum spindle rotation of 60,000 rpm, 3 axes with a resolution of the positioning of 0.1 µm. It was installed on an inertial table, specially designed to reduce the influence of vibrations from external sources during the tests. All experiments and measurements were carried out in a controlled environment at 20 °C.

Blaser's Vascomill MMS FA 2 cutting fluid was used in a minimum quantity fluid (MQF) regime at a pressure of 6 bar. The positioning of the fluid nozzle was at an approximate distance of 10 mm from the microtool and inclination of 20°, as can be seen in Figure 1.

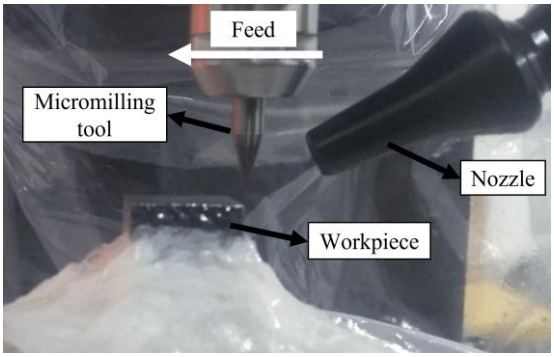

Figure 1. Experimental setup.

The micromilling tools manufactured by Mitsubishi Materials were (Al, Ti)N coated carbide. The tool geometry included two cutting flutes cutting diameter (DC) of 0.4 mm, cutting length (APMX) of 0.8 mm, diameter (DCON) and length (LF) of 4 mm and 40 mm, respectively and radius of the cutting edge of 3.4 µm. Figure 2 illustrates the microtools and identification of each geometric parameter. It is important to emphasize that two tools were used to carry out the tests, one for the hot-rolled sample and another for the LDED sample.

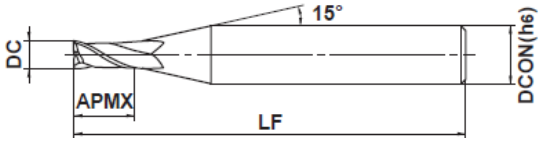

Figure 2 - Geometric parameters of microtools (Mitsubishi, 2021).

The cutting condition used in the tests is shown in Table 3.

Table 3. Cutting parameters.

Cutting speed (m/min)	Feed per tooth (µm/ tooth)	Feed rate (mm/min)	Axial depth of cut (µm)
12.56	10	100	40

The Taylor Hobson® profilometer, model Form Talysurf Intra, was used to measure the surface roughness. The probe scanned near center and along a micromilled channel. Three measurements were obtained in different regions of each microchannel, using a Gaussian filter, cut-off of 0.8 mm, and evaluation length of 4 mm, according to ISO 4288 (1996). For analysis, the average of these measurements and the standard deviation were calculated. The parameter analyzed was the mean arithmetic deviation (Ra).

During the fabrication of each microchannel, the machining force in x-direction was acquired with a data acquisition system. Therefore, the machining force was acquired in the direction perpendicular to the cutting direction, since the objective was to analyze the highest value of the cutting force, which corresponds to the peaks of the acquired force, corresponding to the force obtained in the maximum uncut chip thickness (h_{cu}), as represented in Figure 3. Kistler 9265B dynamometer with a 9443B mounting plate was used to secure and mounted a machined sample. This dynamometer was connected to a Kistler 5407 distribution box, which in turn connected to the Kistler 504E load amplifier. From the amplifier, the signals were sent to the National Instruments NI USB-62211 acquisition board to carry out the conversion from an analog to a digital signal. Finally, the LabView Signal Express software was used to read the digital signal. Figure 4 shows how this signal acquisition system was assembled.

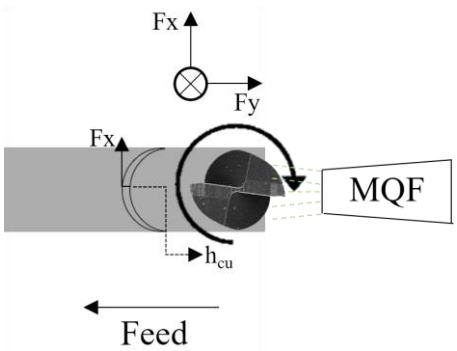

Figure 3. Representation of the acquired cutting force.

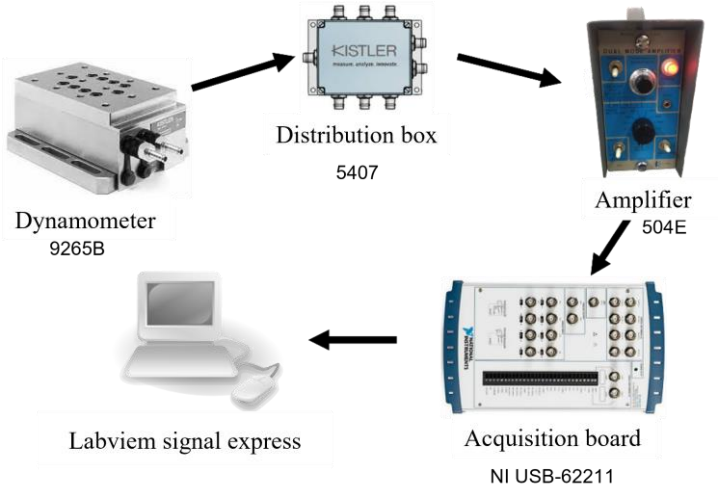

Figure 4. Analyzed force acquisition system.

The Kistler 9265B dynamometer was used in this study. Preliminary experiment found insignificant force difference between this model and that from the mini-dynamometers. The acquired signals were filtered with a low-pass filter of 1000 Hz. This frequency was defined to ensure the presence of 3 times the frequency of tooth passage. In addition, it was necessary to remove a DC level from the raw signal acquired, so that there would be no statistical difference between the values of the cutting force obtained by this dynamometer and the mini-dynamometer.

In the analysis of the acquired force, the mean force of the peaks of the signals collected during the machining period was used, since the peak of the signals of the Fx component corresponds to the highest value of the cutting force for the maximum uncut chip thickness. Matlab was the software used to process the signals. The acquisition rate was 10 kHz.

To measure the wear of the microtool when machining the last microchannel, the microtools were observed in the SEM, using the Scanning Electron Microscope (SEM), from Hitachi High-Technologies model TM3000, for analysis and obtaining images. It is important to emphasize that images of the new microtools were also obtained to verify the existence of any defects in them. The wear was obtained by analyzing the images of the secondary flank face images (top images) of the micromills and for its measurement the images of the new microtool were superimposed on the images of the used ones, using Adobe Photoshop CC software. Then, the wear was measured with Image J software, being established for each of the two cutting flutes, as the distance between the tip of the new and worn tool cutting edge, as schematized in Figure 5.

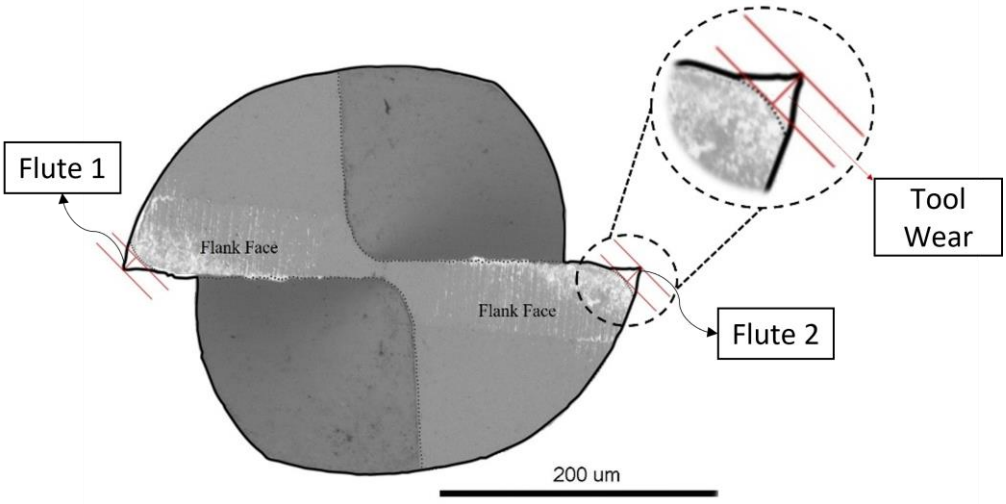

Figure 5. Tool wear measurement (Gomes et al., 2020).

3. RESULTS AND DISCUSSIONS

Figure 6 presents the average arithmetic deviation values (Ra) for each microchannel manufactured in the analyzed samples.

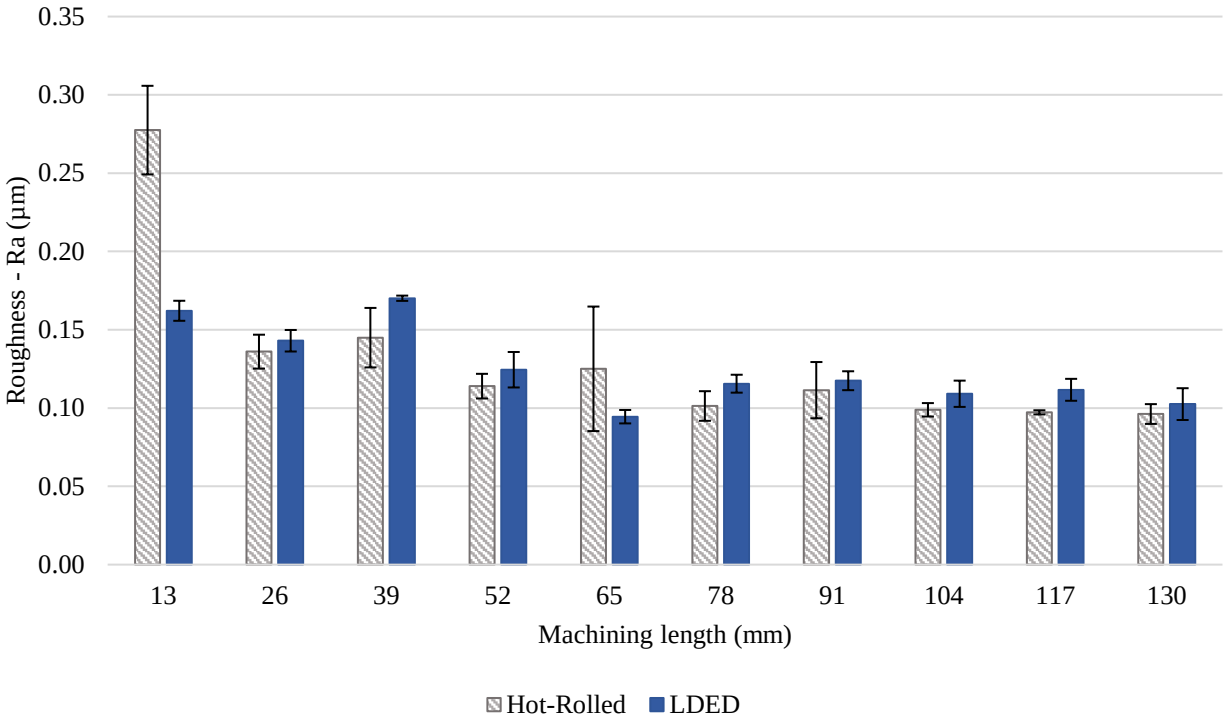

Figure 6. Effect of milling distance on surface finish.

When observing the behavior of the roughness Ra in Figure 6, it is noticed a tendency of reduction with the increase of the machining length. This reduction in roughness can be observed when comparing the images of the surfaces machined in the first and last microchannel, as shown in Figure 7. It is noted that the surface of the first channel has much more evident marks feed per tooth of the micromill compared to the surface of the last channel. This is due to the geometrical changes of cutting edges of the micromill as it wears out. It is suggested that due to wear, the tool showed rounding of the nose radii and flattened cutting edges, therefore, reducing surface roughness, as shown in Figure 8 (Santos et al., 2015; Russell et al., 2022). As shown in Figure 8, the cutting edge radius of new microtools is approximately 3.4 µm, while that of the worn microtools, after machining 130 mm of length, is approximately 9.4 µm and 9.0 µm for the hot-rolled and LDED samples, respectively. Since the values of the cutting edge radius(r_ε) are close to the feed per tooth (f_z = 10 µm/tooth) and the ratio f_z/r_ε is slightly greater than 1, then it is postulated that shear mechanism rather than plowing is the dominant mechanism. In this case, the surface roughness decreases as the f_z/r_ε ratio decreases up to a length of 130 mm, as occurs in conventional machining processes on a macro scale. The values of f_z and r_ε close for the last machined length indicate that after this length (130 mm) the roughness values would increase with each manufactured microchannel, as observed by Krishnan and Mathew (2020), since from this length the ratio f_z/r_ε would be less than 1, being the presence of plowing dominant, leading to the formation of a machined surface with a worse finish.

The differences of feed marks in each analyzed sample can be observed. In the hot-rolled material, the feed marks on first channel (Figure 7 a) and side burrs are more visible than those after 130 mm of the last channel (Figure 7b). Similar trends are seen for the LDED samples (Figure 7 c-d). A tool with higher wear burnishes on the on harder LDED surface and reduces the surface roughness.

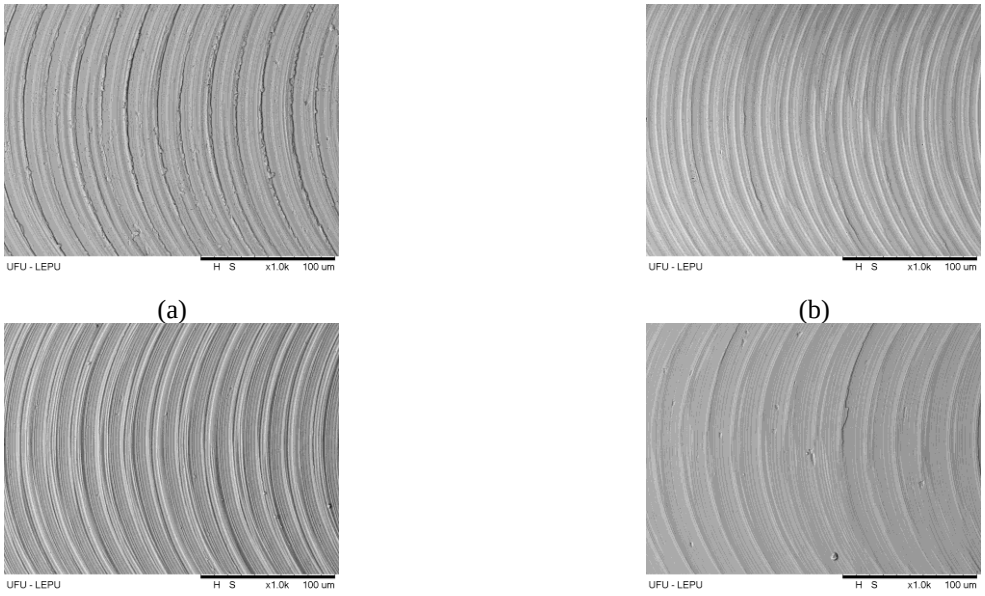

(a) (b)

(c) (d)

Figure 7. Micromachined surface of (a) first channel and (b) last channel of hot-rolled sample and micromachined surface of (c) first channel and (d) last channel of LDED sample.

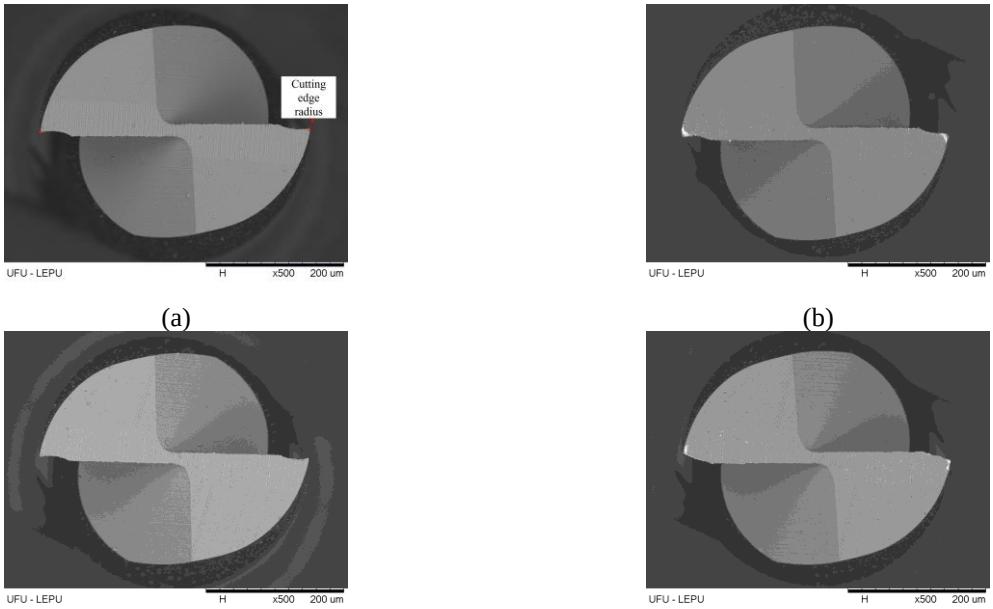

(a) (b)

(c) (d)

Figure 8. Comparison of (a) new microtool and (b) after machining the last microchannel for the hot-rolled sample and (c) new microtool and (d) after machining the last microchannel for the LDED sample.

Tool wear for both cutting flutes are compared in Figure 9. The measurement confirms that the wear of the microtool was greater when micromachining the LDED sample due to its higher hardness. Therefore, this result agrees with the hardness property of the analyzed samples in Table 2.

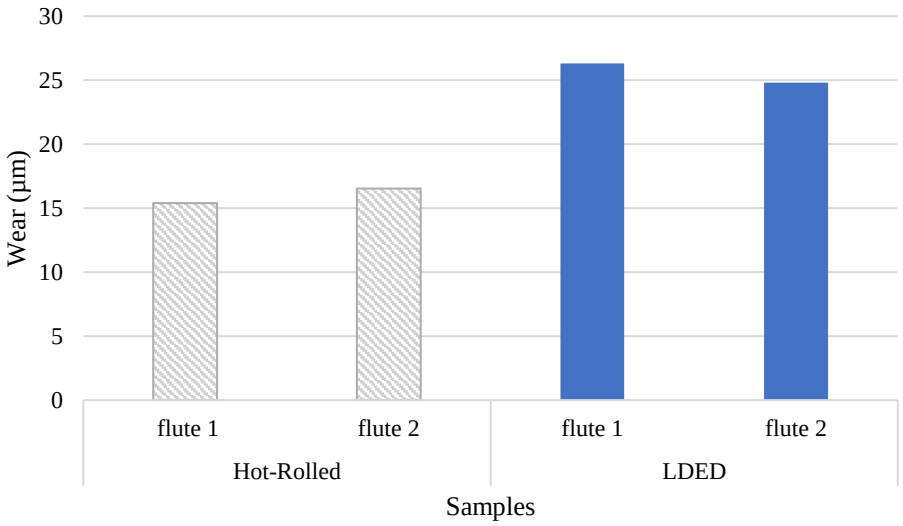

Figure 9. Wear on each flute of the microtool after machining the last channel (after 130 mm milling distance) of the samples manufactured by hot rolling and LDED.

In addition, it can be seen in Figure 6 that small values were found for Ra, ranging from 0.0962 µm to 0.2775 µm, and these values are even smaller than the roughness range determined by Diniz, Marcondes, and Copinni (2010) for grinding processes, which varies from 0.2 µm to 1.6 µm. Although lower surface finish is obtained due to smearing and rubbing of worn tools on the machined surface, high residual stress and plastically deformed grains are expected in the subsurface.

Regarding the Ra values for the two analyzed samples, Figure 6, it is noted that there are no statistical differences between the values obtained for hot-rolled and LDED samples as shown with the overlapping of standard deviations associated with each measurement. This behavior differs only for the machined lengths of 13 mm and 117 mm, requiring further investigations, to better understand this result. This result is in line with that obtained by Gonçalves (2022) when performing the micromilling of titanium alloy Ti-6Al-4V manufactured by selective laser melting (SLM) and by Gomes (2022) in the micromilling of stainless steel 316L manufactured by LDED. However, in some studies carried out, such as by Hojati et al. (2020) who evaluated the micromilling of titanium alloy Ti-6Al-4V manufactured by electron beam melting (EBM), the authors observed that the roughness of the sample manufactured by additive manufacturing is lower than the roughness of the sample manufactured conventionally. The explanation for this result is related to the hardness of the sample, with the roughness of the sample manufactured by additive manufacturing being lower due to its greater hardness compared to the conventional sample. According to these authors, as the hardness of the sample manufactured by the additive manufacturing is greater, that is, the more brittle characteristics of these samples, will mean that during chip formation a smaller amount of material will be pressed material through the ploughing, therefore, a thinner surface will be obtained.

Figure 10 shows the cutting force as a function of the machined length for both samples. It is observed in Figure 10 a tendency to increase the cutting force with the machining length. This occurs due to the wear of the microtool increasing with each machined microchannel (Machado et al., 2011), as can be seen in Figure 8. It is also noted that the standard deviation of the cutting force for the two samples coincide, demonstrating that there are no statistical differences between the values obtained. This result is in line with that found by Gonçalves (2022) when micromilling the titanium alloy Ti-6Al-4V manufactured by selective laser melting (SLM) and by Gomes (2022) in the micromilling of stainless steel 316L manufactured by LDED. However, this behavior differs from that obtained by Oliveira Campos et al. (2020), who analyzed the micromilling of the SLM'ed Ti-6Al-4V alloy and observed that the cutting force was greater for the samples manufactured conventionally, even with lower hardness. In another study by Montevecchi et al. (2016), the authors concluded that milling H13 steel manufactured by Laser-Engineered-Net-Shaping (LENS) and Wire-Arc-Additive-Manufacturing (WAAM) resulted in an increase in the cutting forces for both samples manufactured by additive manufacturing, due to the greater hardness of these materials. Perhaps such contradicting results were due to different tooling and process parameters in respected studies.

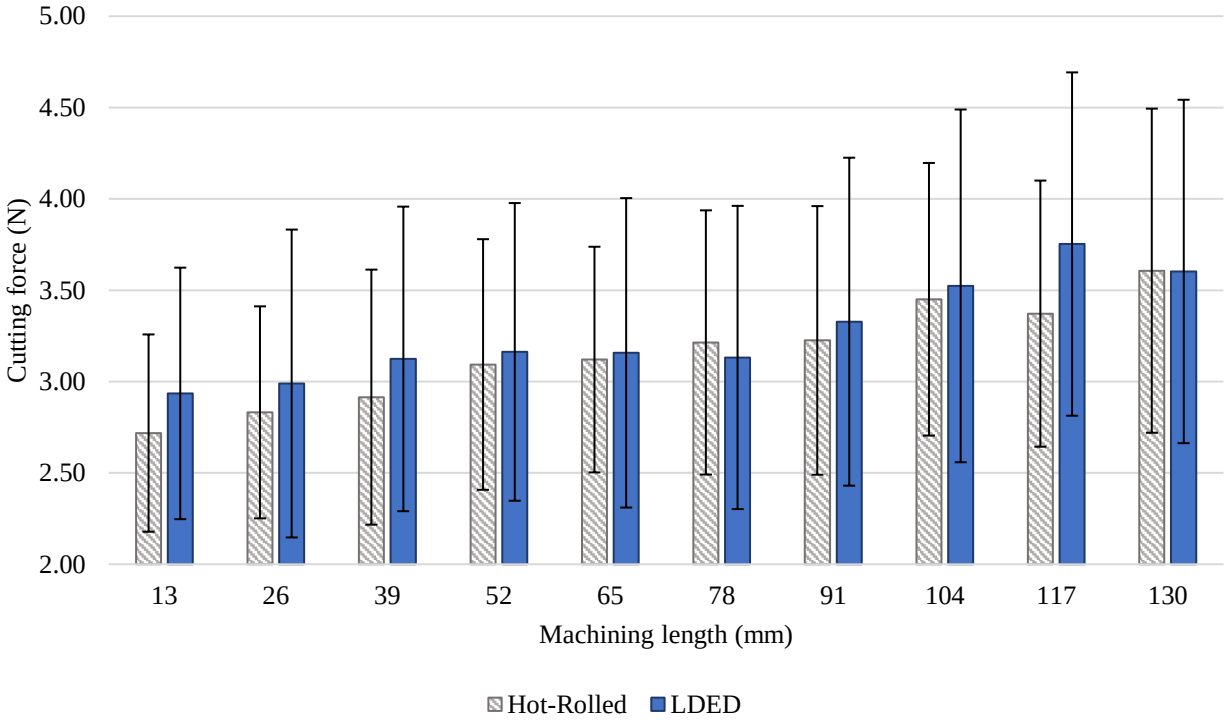

Figure 10. Effect of milling distance on cutting force.

4. CONCLUSIONS

Micromilling of H13 tool steel fabricated by hot-rolled and LDED routes was investigated. The study showed:

i. The surface finish of micromilled channels Ra tended to decrease with increasing machining length. This occurred due tool wear that increased the cutting edge radius of the microtool that reached the value of the feed per tooth, with the cutting being dominated by shear mechanism.
ii. Rubbing of worn out tools produced low submicron surface finish Ra, but may result in plastically deformed subsurface grains and high residual stresses.
iii. The measured cutting force increaseed with the machining length, due to the increasing tool wear.
iv. There were no statistical differences between the Ra values and the cutting force obtained for the machined samples. However, the tool wears were 15-17 µm after milling hot-rolled sample, and 25-26µm after milling the LDED sample. The increase of tool wear was due to increase of corresponding harness 204 VHN of hot-rolled material comparing to 513 VHN of LDED material.
v. In future work, the relationship between cutting force and wear and surface roughness will continue to be investigated through statistical analysis using an analysis of variance.

5. ACKNOWLEDGEMENTS

The authors are grateful to the Graduate Program in Mechanical Engineering at the Federal University of Uberlândia, to Federal Agency for the Support and Improvement of Higher Education (CAPES), National Council for Scientific and Technological Development (CNPq), award numbers: 151091/2022-6, and Minas Gerais State Research Foundation (FAPEMIG), for financial support. We also thank the organizing committee of the 12th Brazilian Congress of Manufacturing Engineering.

6. REFERENCES

Aramcharoen, A., Mativenga, P.T., Yang, S., Cooke, K.E., Teer, D.G., 2008. Evaluation and selection of hard coatings for micro milling of hardened tool steel. International Journal of Machine Tools & Manufacture. Vol. 48, p. 1578 – 1584.

Asnafi, N., 2021. Tool and Die Making, Surface Treatment, and Repair by Laser-based Additive Processes. *BHM Berg- und Hüttenmännische Monatshefte*, Vol. 166, p. 225-236.

Câmara, M. A., Rubio, J. C., Abrão, A. M., Davim, J. P., 2012. State of the art on micromilling of materials, a review. Journal of Materials Science & Technology. Vol. 28, n. 8, p. 673-685.

Cheng, K. e Huo, D., 2013. Micro-Cutting – Fundamentals and Applications. Ed. Wiley, United Kingdom, 366p.
Diniz, A.E., Marcondes, F.C., Coppini, N.L., 2008. Tecnologia da Usinagem dos Materiais, 6ª edição, Editora Artliber.
Gomes, M. C., da Silva, M. B., Duarte, M. A. V., 2020. Experimental study of micromilling operation of stainless steel. The International Journal of Advanced Manufacturing Technology, Vol. 111, n. 11, p. 3123-3139.
Gomes, M. C., 2022. Study of the Micromilling Process in Stainless Steel ABNT 316L Produced by Casting and Additive Manufacturing. 2022. Doctoral thesis, Federal University of Uberlandia - MG.
Gomes, M.C., Dos Santos, A.G., De Oliveira, D., Figueiredo, G.V., Ribeiro, K.S.B., Los Rios, D, Da Silva, M.B., Coelho, R.T., Hung, W. N., 2021. Micro-machining of additively manufactured metals: a review, The International Journal of Advanced Manufacturing Technology, p. 1-20.
Gonçalves, M.C.C., 2022. Experimental Investigation On Micromilling Machining Of TI-6AL-4V Titanium Alloy Additively Manufactured By Selective Laser Melting (SLM). Master´s Dissertation, University of Sao Paulo - SP.
Hojati, F., Daneshi, A., Soltani, B., Azarhoushang, B., Biermann, D., 2020. Study on machinability of additively manufactured and conventional titanium alloys in micro-milling process. Precision Engineering, Vol. 62, p. 1-9.
Hung, W. N. P, Corliss, M., 2019. Micromachining of Advanced Materials. In: Micromachining. IntechOpen.
Krishnan, A.N., Mathew, J., 2020. Studies on wear behavior of AlTiN-coated WC tool and machined surface quality in micro endmilling of Inconel 718. The International Journal of Advanced Manufacturing Technology. Vol. 110, p. 291-307.
Kumbhar, N. N. e Mulay, A. V., 2018. Post processing methods used to improve surface finish of products which are manufactured by additive manufacturing technologies: a review. Journal of The Institution of Engineers (India): Series C. Vol. 99, n. 4, p. 481-487.
Liu, K. e Melkote, S. N., 2007. Finite element analysis of the influence of tool edge radius on size effect in orthogonal micro-cutting process. International Journal of Mechanical Sciences". Vol. 49, p. 650–660.
Machado, A. R., Abrão, A. M., Coelho, R. T., Da Silva, M. B., 2011. Teoria da Usinagem dos Materiais, Edgard Blucher, São Paulo.
Mitsubishi, 2021. "Mitsubishi Carbide". 3 Jan. 2021. <https://www.mitsubishicarbide.com/mmus/catalog/pdf/lj/lj403a.pdf>.
Montevecchi, F., Grossi, N., Takagi, H., et al., 2016. Cutting Forces Analysis in Additive Manufactured AISI H13 Alloy", Procedia CIRP, Vol. 46, p. 476.
Oliveira Campos, F., Araujo, A.C., Munhoz, A.L.J., Kapoor, S.G., 2020. The influence of additive manufacturing on the micromilling machinability of Ti6Al4V: A comparison of SLM and commercial workpieces. Journal of Manufacturing Processes, Vol. 60, p. 299-307.
Rodrigues, A. R., Jasinevicius, R. G., 2017. Machining scale: Workpiece grain size and surface integrity in micro end milling. In: Microfabrication and Precision Engineering, p. 27-68.
Russell A., Suri S.B., Ribeiro K.S.B., Coelho R.T., De Freitas S.A., Gomes M.C., Da Silva M.B., De Oliveira D., Hung N.W., 2022. Micromilling H13 Tool Steel and Tool Life Criteria for Coated Microtools., 2022. 5th World Congress on Micro and Nano Manufacturing (WCMNM 2022). Leuven, Belgium, September, 2022.
Salonitis, K., D'Alvise, L., Schoinochoritis, B., Chantzis, D., 2016. Additive manufacturing and post-processing simulation: laser cladding followed by high speed machining. The International Journal of Advanced Manufacturing Technology. Vol. 85, n. 9-12, p. 2401-2411.
Santos, A. G., Cunha, D. F., Ziberov, M., Hung, W. N., Jackson, M. J., Da Silva, M. B., 2015. Avaliação Da Qualidade De Microcanais Fabricados Por Microfresamento No Aço Inoxidável Duplex Uns 32205, Anais do 8º Congresso Brasileiro de Engenharia de Fabricação.
Serje, D., Pacheco, J., Diez, E., 2020. Micromilling research: Current trends and future prospects. The International Journal of Advanced Manufacturing Technology, Vol. 111, n. 7, p. 1889-191.
Simoneau, A., Ng, E., Elbestawi, M.A., 2006. Chip Formation during microscale cutting of a medium carbon steel. International Journal of Machine Tools & Manufacture: Design, Research and Application. Vol. 46, n. 5, p. 467-481.
Yi, L., Gläßner, C., Aurich, J. C., 2019. How to integrate additive manufacturing technologies into manufacturing systems successfully: A perspective from the commercial vehicle industry. Journal of Manufacturing Systems, Vol. 53, p. 195-211.
Zhai, Y., Lados, D. A., Lagoy, J. L., 2014. Additive manufacturing: making imagination the major limitation. Jom, Vol. 66, n. 5, p. 808-816.
Zhang, Y., Jarosinski, W., Jung, Y. G., Zhang, J., 2018. Additive manufacturing processes and equipment. In: Additive Manufacturing. Butterworth-Heinemann, p. 39-51.

7. RESPONSIBILITY NOTICE

The authors are the only responsible for the printed material included in this paper.